Materials Research Express

PAPER

Simulating stress-tunable phonon and thermal properties in heterostructured AlN/GaN/AlN-nanofilms

Xiaoya Tang[1], **Jiachuan Wang**[1], **Linli Zhu**[1] **and Wenyan Yin**[2]

[1] Department of Engineering Mechanics, and Key Laboratory of Soft Machines and Smart Devices of Zhejiang Province, Zhejiang University, Hangzhou 310027, People's Republic of China

[2] Innovative Institute of Electromagnetic Information and Electronic Integration, College of Information Science and Electronic Engineering, and Key Laboratory of Micro-Nano Electronics and Smart Systems of Zhejiang Province, Zhejiang University, Hangzhou 310027, People's Republic of China

E-mail: llzhu@zju.edu.cn

RECEIVED
20 July 2018

REVISED
29 August 2018

ACCEPTED FOR PUBLICATION
25 September 2018

PUBLISHED
10 October 2018

Keywords: AlN/GaN/AlN nanofilms, phonon properties, phonon thermal conductivity, elastic model, prestress fields

Abstract

The acoustic phonon and thermal properties of GaN-based heterostructured nanofilms are investigated theoretically considering the effects of quantum confinement and prestress fields. The continuum elastic model is utilized to derive the acoustic phonon dispersion relations of GaN-based nanofilms in which the prestress fields are taken into account. The numerical results demonstrate that prestress fields can alter acoustic phonon properties significantly, such as dispersion relation and phonon group velocities. The trend of variation turns to be opposite as the direction of prestress fields reverses. The change of phonon properties under various prestress fields is sensitive to the thickness of core layer in heterostructured nanofilms. Moreover, the modification of acoustic phonon properties in heterostructured nanofilms under prestress fields gives rise to the change of phonon thermal conductivities for different phonon modes. Moreover, prestress fields can modify the influence of temperature-dependent phonon thermal conductivity of GaN-based heterostructured nanofilms. The results in this work could be helpful for the thermal management and rational design of high-performance in nano/microelectronic devices.

1. Introduction

Semiconductor-based electronic devices are widely applied in modern technology, which have been one of the fastest developing fields over the past half century. With the demands of calculation speed, efficiency, economy and portability, the miniaturized, integrated and functional electronic devices have been extensively used, such as integrated circuits, widely used computer circuits and memory, and field effect transistors, light-emitting diodes, and three-dimensional stacking chips [1–4]. As the characteristic sizes of semiconductor devices reduce from micron scale to nanometer level, thermal dissipation becomes the key problem that restricts the performance, service life and reliability of devices [5–8], which requires the high thermal conductivity for the efficient heat dissipation. For thermoelectric materials used in solid-state compact refrigerators and coolers [5, 9–12], the efficiency of thermoelectric conversion is proportional to the dimensionless thermoelectric figure of merit (ZT), known as $ZT = \sigma S^2/\kappa$ [13–15]. Here, $\kappa = \kappa_e + \kappa_{ph}$ is thermal conductivity. Semiconductors with low thermal conductivity are preferred for higher thermoelectric conversion efficiency [16, 17]. Hence, thermal conductivity plays an essential role in the performance of semiconductor-based nanoelectronic devices. Since phonon thermal conductivity dominates the thermal conductivity in semiconductors, it is necessary to study the phonon thermal conductivity.

In practical applications, semiconductor-based electronic devices exist mostly in multilayered heterostructures, for example, edge-emitting lasers [17–19], heterojunction bipolar transistors for microwave and low-power wireless communications [20, 21] and high electron mobility transistors (HEMTs) [22, 23]. To study the phonon and thermal properties of semiconductor heterostructures is one of the hot topics in last

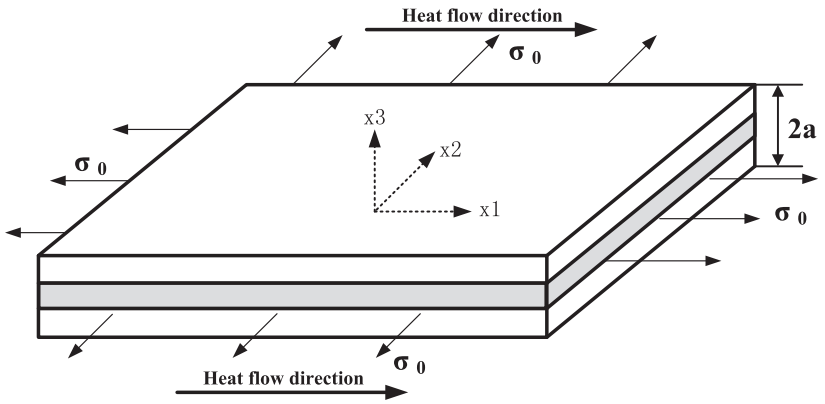

Figure 1. GaN-based heterostructured nanofilm with in-plane prestress. The darker part refers to GaN, and the white part represents AlN.

several tens of years. Understanding the thermal conductivity of heterogeneous nanostructures is critical for the development of nano/microelectronics and optoelectronic devices [5, 17]. Superlattice structures based on InAs/AlSb are widely used in high-speed field effect transistors (FETs), infrared detectors and diode lasers. Borca-Tasciuc *et al* [24] measured the variation of in-plane thermal conductivity of InAs/AlSb superlattice in the range of 80–300 K using 3ω method. The thermal conductivity measured in experiment is about an order of magnitude lower than the bulk value. Moreover, lower thermal conductivity mostly occurs in samples grown at high temperature and samples annealed, which is probably due to the increase of interfacial roughness and phonon interface reflection caused by high growth temperature and annealing. According to the Boltzmann transport equation, Zeng *et al* [25] established a unified model for nonequilibrium electron, nonequilibrium phonon and the nonequilibrium condition between phonon and electron in a double heterojunction. They calculated the variation of equivalent thermoelectric parameters such as Seebeck coefficient along with the film thickness in silicon-based heterojunctions. Nika *et al* [26–28] utilized the face centered cubic (FCC) cell dynamic lattice model to study the lattice heat flow in three-layered heterogeneous nanofilms with silicon or germanium as the core layer. It was found that the acoustic mismatched cladding material has a remarkable contribution on phonon dispersion and heat flux in heterostructures. They also calculated the change of acoustic phonon properties and lattice thermal conductivity with temperature in heterostructured wires of rectangular cross-section, and found that cladding material with higher (lower) acoustic velocity could increase (decrease) the phonon thermal conductivity of nanostructure, which illustrates the feasibility of adjusting the elastic constants and sizes of cladding materials to regulate the phonon and thermal characteristics. Narendra and Kim [29] studied the influence of heterogeneous interfaces on thermoelectric properties in P-type Bi_2Te_3/Sb_2Te_3 heterojunction. A fully first-principles atomistic approach and Monte Carlo model was used to calculate the interfacial thermal impedance and the electron transport characteristics. It turns out that the interfacial thermal impedance and local increase of power factor strengthen the overall thermal performance of heterojunction, and the value of ZT can be magnified significantly in the case of geometric optimality. Pokatilov *et al* [30] calculated the phonon dispersion relation and phonon group velocity of AlN/GaN/AlN heterostructures and proved theoretically that the phonon group velocity could be changed by adjusting the parameters and thickness of cladding materials thus the thermal performance of semiconductor heterostructures could be optimized.

Stress field is often introduced in semiconductor devices due to industry produce [31–33] or temperature variation [34, 35]. Stress or strain can change the performance parameters such as thermal conductivity, leading to affecting the safety and stability of devices. On the other hand, to tune the phonon properties through applying stress or strain fields could be regarded as one of the phonon engineering approaches. Ross *et al* [36] concluded that the thermal conductivity increases with compressive stress (strain), which is possibly due to the enlargement of phonon group velocity under compression. A modified Keating/VFF (valence-force-field) model was developed by Sui and Herman [37] for the calculation of Phonon dispersion relations of bulk Si, Ge and their strained layers, and Si/Ge superlattice nanofilms under external stress and hydrostatic pressure. The computing results are in good agreement with existed experimental results. This model can be applied to other crystal materials with diamond structure and zinc-blende materials in III–V and II–VI family after proper modification. Analogously, Ghanbari *et al* [38] proposed a modified six-parameter valence-force-potential model to simulate the phonon characteristics of Si/Ge layered superlattices under strain field. In the work of Li *et al* [39], the lattice thermal conductivity of single-walled Si nanowire and monolayer graphene were calculated by equilibrium molecular dynamics simulation, which was found to decrease continuously with the

strain from negative to positive. This phenomenon is caused by change of phonon dispersion relation under stress field, and the variation of thermal conductivity in single-walled nanotube can be as high as 130% under strain field. Bhowmicka and Shenoy [40] determined the temperature and strain dependence of phonon relaxation time using Fermi golden rule and classical molecular dynamics simulations, which reveals the mechanism of strain field changing the phonon velocity and relaxation time, thus affecting the thermal conductivity. Paul and Klimeck [41] applied a modified VFF model to investigate the effect of uniaxial stress and hydrostatic pressure on ballistic thermal conductance of Si nanowire and specific heat. Their results show that the thermal conductivity appears to be anisotropic under stress field, but the specific heat exhibits isotropy. Furthermore, uniaxial stress can be used to control thermal conductivity under low stress. Based on the continuum theory, Zhu *et al* investigate the phonon thermal conductivity of quantum confined Si nanofilm [42], homogeneous and heterogeneous structures of GaN [43–45]. It was found that stress can remarkably change the thermal conductivity of nanostructures, and the response of which to temperature and physical size can also be affected by stress. Picu *et al* [46] obtained a similar result by studying the influences of strain and size effect on heat transfer in nanostructures, using a molecular dynamics simulation of Lennard-Jones solid model. That is, tensile (compressive) strain leads to decrease (increase) of lattice thermal conductivity. They found that the effect is caused by the variation of stiffness matrix and lattice anharmonicity along with strain, which further leads to changing the phonon group velocity and phonon mean free path. Tailoring phonon mean free path was suggested to be used as an indirect approach to control the size effect.

Previous researches about the effect of stress/strain field on thermal properties are mainly focused on bulk materials or nanowires of Si and Ge [36, 37, 47], or carbon based nanotubes and nanofilms [39], and superlattice structures [36, 48–50]. Due to the lack of researches on stressed or constrained heterostructures, it is necessary to investigate the effect of stress field on thermal conductivity in heterostructured nanofilms. In this work, the phonon and thermal properties of AlN/GaN/AlN nanofilm were calculated under the effects of quantum confinement and prestress fields. The acoustoelastic theory is adopted to figure out phonon dispersion relation and group velocity with different thickness and prestress. Then, the variation of phonon thermal conductivity with prestress fields is calculated. The stress effects on phonon and thermal properties in heterostructured nanofilm are systematically explored. This work will be helpful for phonon engineering in efficient thermal management and precise design of nano/microelectronic devices.

2. Theoretical model

2.1. Spatially confined phonons in stressed AlN/GaN/AlN-nanofilms

Since the thermal properties in semiconductor nanostructures are mainly associated with the acoustic phonons. It has been proved that the acoustic phonons with spatial confinement effect can be described by the elastic model [51–55]. Thereby, the continuum elasticity model is utilized to characterize the acoustic phonon properties in heterostructured nanofilms, taking a three-layered AlN/GaN/AlN nanofilm as the example as shown in figure 1. Assume that the nanofilm is subjected to in-plane biaxial prestresses σ_{ij}^0, the corresponding prestrains can be written as u_{ij}^0. The stress-strain relationship in initial state of the orthotropic nanofilm satisfies:

$$u_{ij}^0 = s_{ijkl}\sigma_{kl}^0 \text{ or } \sigma_{ij}^0 = c_{ijkl}u_{kl}^0. \tag{1}$$

Here, $u_{ij}^0 = (\partial u_i^0/\partial x_j + \partial u_j^0/\partial x_i)/2$. Therefore, the acoustoelastic vibration equation of the orthotropic nanofilm can be obtained,

$$\rho^{new}\frac{\partial^2 u_i}{\partial t^2} = \frac{\partial}{\partial x_j}\left[\sigma_{ij} + \sigma_{jk}^0\frac{\partial u_i}{\partial x_k}\right]. \tag{2}$$

In which, $\rho^{new} \approx \rho(1 - \Delta u^0)$ is the density of nanofilm after deformation, and $\Delta u^0 = u_{11}^0 + u_{22}^0 + u_{33}^0 = \frac{\partial u_1^0}{\partial x_1} + \frac{\partial u_2^0}{\partial x_2} + \frac{\partial u_3^0}{\partial x_3}$. The Hooke's law: $\sigma_{ij} = \widehat{C}_{ijkl}u_{kl} = \widehat{C}_{ijkl}\frac{\partial u_k}{\partial x_l}$.

For the nanofilm under an in-plane biaxially prestress, the initial stresses can be written as:

$$\sigma_{11}^0 = \sigma_{22}^0 = \sigma_0,\ \ \sigma_{3i}^0 = 0. \tag{3}$$

The variable with subscript as 1 or 2 denotes the in-plane direction, whereas a subscript 3 denotes the direction of thickness, which is also the hexagonal axis of AlN and GaN crystals. Thus, the prestrains can be derived as follows:

$$u_{11}^0 = \frac{s_{22} - s_{12}}{s_{11}s_{22} - s_{12}^2}\sigma^0,\ \ u_{22}^0 = \frac{s_{11} - s_{12}}{s_{11}s_{22} - s_{12}^2}\sigma^0,\ \ u_{33}^0 = -\frac{c_{13}}{c_{33}}u_{11}^0 - \frac{c_{23}}{c_{33}}u_{22}^0. \tag{4}$$

in which, $s_{11} = c_{11} - c_{13}^2/c_{33}$, $s_{12} = c_{12} - c_{13}c_{23}/c_{33}$, $s_{22} = c_{22} - c_{23}^2/c_{33}$. The acoustoelastic vibration equation in the stressed heterofilm can be expressed as:

$$\rho^{new}(x_3)\frac{\partial^2 u_i}{\partial t^2} = \frac{\partial}{\partial x_j}\left(\widehat{C}_{ijkl}(x_3)\frac{\partial u_k}{\partial x_l}\right) + \sigma^0\frac{\partial^2 u_i}{\partial x_1^2}. \tag{5}$$

$\widehat{C}_{ijkl}$ represents the modified second-order modulus, given by:

$$\widehat{C}_{ijkl} = c_{ijkl}(1 + u^0_{ii} + u^0_{jj} + u^0_{kk} + u^0_{ll} - u^0_{11} - u^0_{22} - u^0_{33}) + c_{ijklmn}u^0_{mn}. \tag{6}$$

Applying the general rule of subscript simplification, the non-zero modulus can be expressed as below:

$$\begin{aligned}
&\widehat{C}_{11} = \widehat{C}_{22} = c_{11}(1 + 2u^0_{11} - u^0_{33}) + (c_{111} + c_{112})u^0_{11} + c_{112}u^0_{33}\\
&\widehat{C}_{33} = c_{11}(1 + 2u^0_{11} - u^0_{33}) + 2c_{112}u^0_{11} + c_{111}u^0_{33}\\
&\widehat{C}_{13} = \widehat{C}_{23} = c_{12}(1 + u^0_{33}) + (c_{123} + c_{112})u^0_{11} + c_{112}u^0_{33}\\
&\widehat{C}_{12} = c_{12}(1 + u^0_{33}) + 2c_{112}u^0_{11} + c_{123}u^0_{33}\\
&\widehat{C}_{44} = \widehat{C}_{55} = c_{44}(1 + u^0_{33}) + (c_{144} + c_{155})u^0_{11} + c_{155}u^0_{33}\\
&\widehat{C}_{66} = (\widehat{C}_{11} - \widehat{C}_{22})/2.
\end{aligned} \tag{7}$$

Owing to the heterogeneity of the structure, the density and elastic modulus vary with film thickness, which satisfy the rule below:

$$\rho^{new}(x_3) = \begin{cases} \rho^{new}{}_{AlN}, & -\frac{t_{GaN}}{2} - t_{AlN} \leqslant x_3 \leqslant -\frac{t_{GaN}}{2} \\ \rho^{new}{}_{GaN}, & -\frac{t_{GaN}}{2} \leqslant x_3 \leqslant \frac{t_{GaN}}{2} \\ \rho^{new}{}_{AlN}, & \frac{t_{GaN}}{2} \leqslant x_3 \leqslant \frac{t_{GaN}}{2} + t_{AlN} \end{cases},$$

$$\overline{C}_{ij}(x_3) = \begin{cases} \overline{C}_{ijAlN}, & -\frac{t_{GaN}}{2} - t_{AlN} \leqslant x_3 \leqslant -\frac{t_{GaN}}{2} \\ \overline{C}_{ijGaN}, & -\frac{t_{GaN}}{2} \leqslant x_3 \leqslant \frac{t_{GaN}}{2} \\ \overline{C}_{ijAlN}, & \frac{t_{GaN}}{2} \leqslant x_3 \leqslant \frac{t_{GaN}}{2} + t_{AlN} \end{cases}. \tag{8}$$

For the equation (5), one can write the solution of displacement as follows:

$$\mathbf{u} = \overline{\mathbf{u}}(x_3)\exp[i(\omega t - q \cdot x_1)]. \tag{9}$$

Here, ω is phonon frequency, and q is the wave vector. $\overline{\mathbf{u}}$ refers to the amplitude of displacement vector. Substituting equation (9) into equation (5), the vibration equation of heterostructured nanofilm under prestress fields can be obtained, given as:

$$\begin{cases} (\widehat{C}_{11}(x_3) + \sigma^0)\frac{\partial^2 u_1}{\partial x_1^2} + \widehat{C}_{44}(x_3)\frac{\partial^2 u_1}{\partial x_3^2} + (\widehat{C}_{13}(x_3) + \widehat{C}_{44}(x_3))\frac{\partial^2 u_3}{\partial x_1 \partial x_3} = \rho^{new}(x_3)\frac{\partial^2 u_1}{\partial t^2} \\ (\widehat{C}_{66}(x_3) + \sigma^0)\frac{\partial^2 u_2}{\partial x_1^2} + \widehat{C}_{44}(x_3)\frac{\partial^2 u_2}{\partial x_3^2} = \rho^{new}(x_3)\frac{\partial^2 u_2}{\partial t^2} \\ (\widehat{C}_{44}(x_3) + \sigma^0)\frac{\partial^2 u_3}{\partial x_1^2} + \widehat{C}_{33}(x_3)\frac{\partial^2 u_3}{\partial x_3^2} + (\widehat{C}_{13}(x_3) + \widehat{C}_{44}(x_3))\frac{\partial^2 u_1}{\partial x_1 \partial x_3} = \rho^{new}(x_3)\frac{\partial^2 u_3}{\partial t^2} \end{cases}. \tag{10}$$

To solve the differential equations in equation (10), the boundary conditions are needed and can be expressed as follows:

$$x_3 = \pm a, \quad \sigma_{13} = \sigma_{23} = \sigma_{33} = 0. \tag{12}$$

Here, $2a$ represents the film thickness. For shear (SH) mode, the film displacement can be written as $\overline{u} = (0, \ u_2, \ 0)$. The eigenvalue equation of SH mode is thus obtained:

$$\widehat{C}_{44}(x_3)\frac{d^2\overline{u}_2}{dx_3^2} + [\rho^{new}(x_3)\omega^2 - (\widehat{C}_{66}(x_3) + \sigma^0)q^2]\overline{u}_2 + \frac{d\widehat{C}_{44}}{dx_3}\frac{d\overline{u}_2}{dx_3} = 0. \tag{13}$$

For the dilatational mode (SA) and flexural mode (SA), the film displacements are $\overline{u} = (u_1, \ 0, \ u_3)$, and then the eigenvalue equations are derived as:

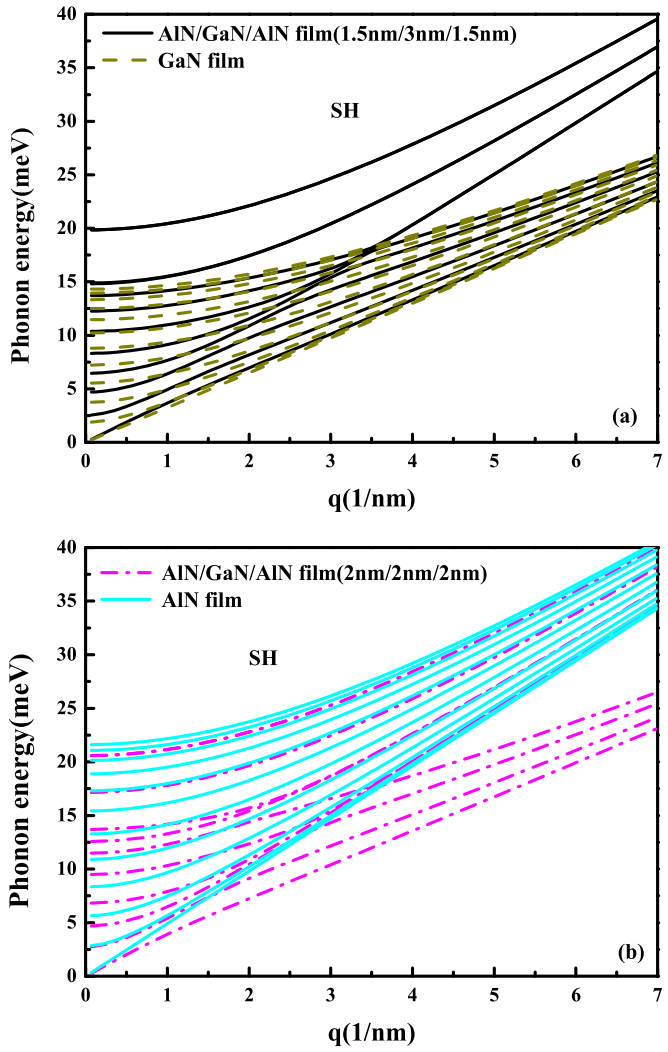

Figure 2. Phonon dispersion relations of SH mode for GaN nanofilm, AlN nanofilms and two typical heterostructured nanofilms.

Table 1. Elastic modulus of AlN/GaN/AlN nanofilms used in this paper.

GaN	C11(GPa)	C13(GPa)	C55(GPa)	C111(GPa)	C123(GPa)
	252	129	148	−1213	−253
	C144(GPa)	C155(GPa)	C112(GPa)	C456(GPa)	ρ(Kg/m^3)
	−46	−606	−867	−49	6100
AlN	C11(GPa)	C13(GPa)	C55(GPa)	C111(GPa)	C123(GPa)
	282	149	179	−1073	−61
	C144(GPa)	C155(GPa)	C112(GPa)	C456(GPa)	ρ(Kg/m^3)
	57	−757	−965	−9	3235

$$\begin{cases} \widehat{C}_{44}(x_3)\dfrac{d^2\overline{u}_1}{dx_3^2} + [\rho^{new}(x_3)\omega^2 - (\widehat{C}_{11}(x_3) + \sigma^0)q^2]\overline{u}_1 + \dfrac{d\widehat{C}_{44}}{dx_3}\dfrac{d\overline{u}_1}{dx_3} \\ \qquad -iq(\widehat{C}_{13}(x_3) + \widehat{C}_{44}(x_3))\dfrac{d\overline{u}_3}{dx_3} - iq\dfrac{d\widehat{C}_{44}}{dx_3}\overline{u}_3 = 0 \\ \widehat{C}_{33}(x_3)\dfrac{d^2\overline{u}_3}{dx_3^2} + [\rho^{new}(x_3)\omega^2 - (\widehat{C}_{44}(x_3) + \sigma^0)q^2]\overline{u}_3 + \dfrac{d\widehat{C}_{33}}{dx_3}\dfrac{d\overline{u}_3}{dx_3} \\ \qquad -iq(\widehat{C}_{13}(x_3) + \widehat{C}_{44}(x_3))\dfrac{d\overline{u}_1}{dx_3} - iq\dfrac{d\widehat{C}_{13}}{dx_3}\overline{u}_1 = 0 \end{cases}. \quad (14)$$

Combining the corresponding boundary conditions and different elastic parameters, the phonon dispersion relations of SH, SA and AS modes could be determined numerically. We know that the interfaces effects could

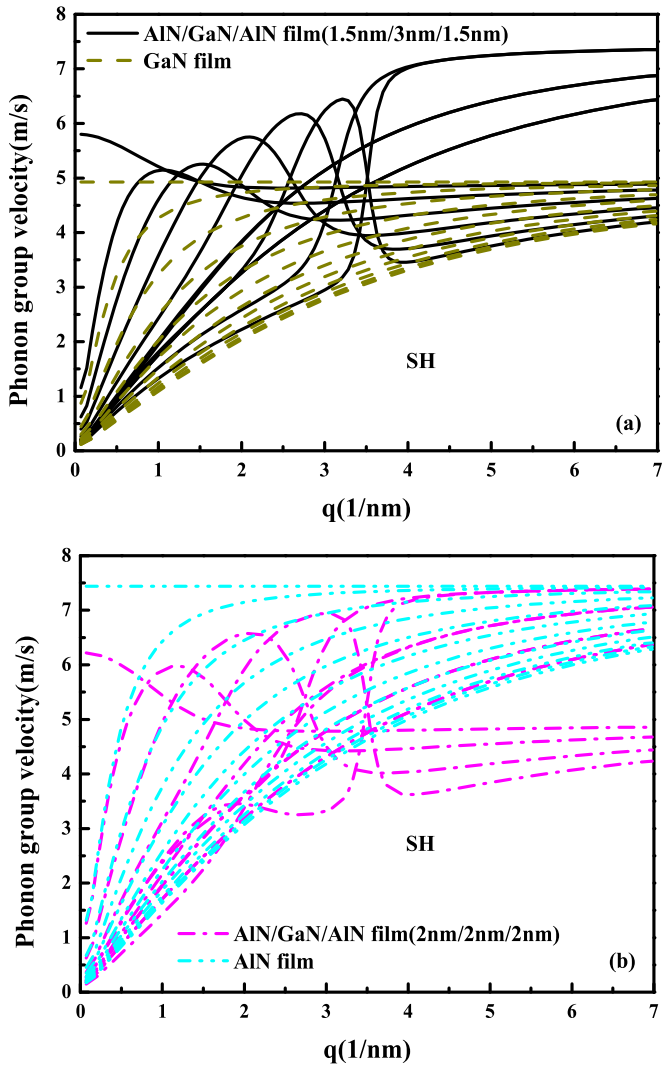

Figure 3. Phonon group velocities of SH mode for GaN nanofilm, AlN nanofilms and two typical heterostructured nanofilms.

contribute to the physical and mechanical performance of nanostructures significantly. For example, the interface/surface phonon scattering could modify the phonon thermal properties, and the surface/interface stress can also affect the phonon properties so as to change the thermal conductivity of nanostructure [44, 55–58]. For convenience in this study, supposed the GaN layer and AlN layer connected perfectly and the influence of lattice mismatch is neglected. The displacement compatibility condition is adopted for the interfaces between GaN layer and AlN layer in simulations.

2.2. Phonon thermal conductivity

As one of the most important characterization of thermal properties in semiconductor nanomaterials, the phonon thermal conductivity is closely related to phonon properties, such as phonon group velocity and the density of states (DOS). The expression of phonon thermal conductivity can be written as follows [54, 55]:

$$\kappa(T) = \frac{1}{3}\left(\frac{k_B}{\hbar}\right)k_B T\sum_n \int \frac{x^2 e^x}{(e^x - 1)^2} f_n(x) v_n^2(x)\tau_n(x)\,dx, \tag{15}$$

in which $x = \hbar\omega/k_B T$. k_B is the constant of Boltzmann. v_n and f_n refer to phonon group velocity and density of states, respectively. τ_n represents the relaxation time of phonon and T is temperature. It should be emphasized that the phonon thermal conductivity in equation (15) involves the conductivities of SH mode, AS mode, and SA modes. Since the wave vector changes from zero to π/d, the integration with respect of frequency in equation (15) is over the entire Brillouin zone.

According to the acoustoelastic model, the phonon dispersion relations of AlN/GaN/AlN nanofilm under different modes have been determined. Based on phonon dispersion relations, the phonon group velocity can be

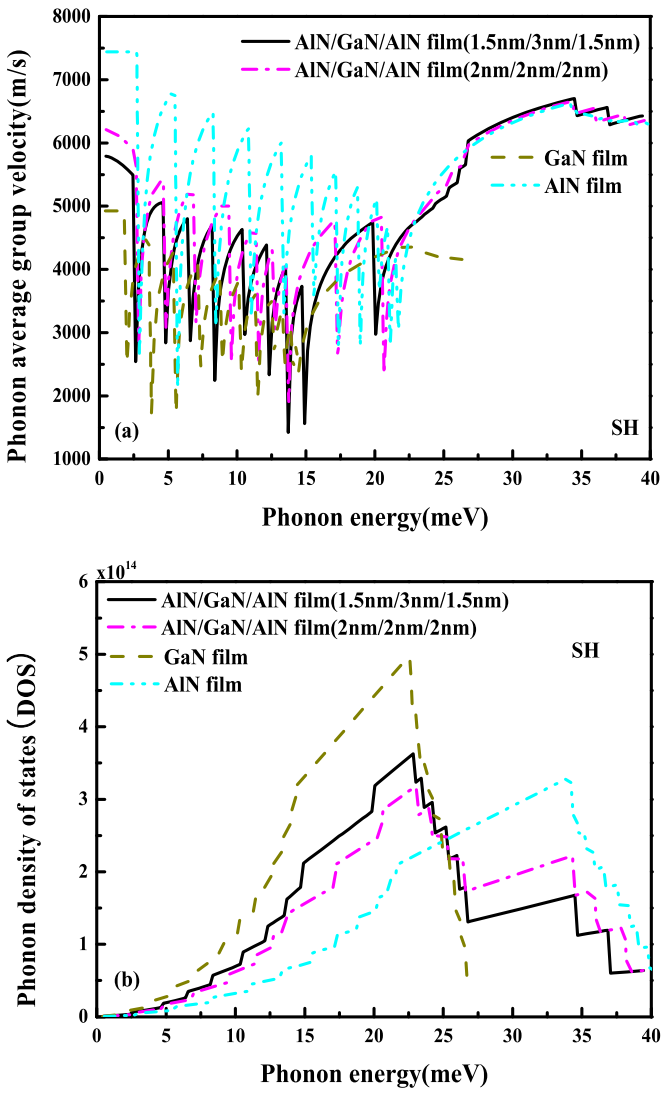

Figure 4. Phonon average group velocities (a) and phonon density of states (b) of SH mode for GaN nanofilm, AlN nanofilms and two typical heterostructured nanofilms.

derived by numerical differentiation:

$$v_n(k) = \frac{d\omega_n(k)}{dk}. \tag{16}$$

The subscript n is the quantum number of modes. Given a polarization, n equals to the ratio $2a/\mathrm{d}$, where $2a$ is the film thickness and d is the lattice constant. To analyze the thermal properties of semiconductor nanomaterials, the number of phonon modes of a unit frequency interval per unit volume is defined as phonon density of states (DOS), which can be written as follows:

$$f_n^{SA,AS,SH}(\omega) = \frac{1}{2a}\left[\frac{1}{2\pi} q_n^{SA,AS,SH}(\omega) \frac{1}{v_n^{SA,AS,SH}}\right]. \tag{17}$$

Here, n refers to number of phonon branch. After calculating the DOS in different modes, the total DOS of nanofilm can be derived as below:

$$F(\omega) = \sum\nolimits_n f_n(\omega). \tag{18}$$

There are many types of phonon scattering mechanisms in semiconductor materials, such as three-phonon scattering, phonon-defect scattering, boundary scattering and phonon-electron scattering. In this work, suppose that the surfaces/interfaces of heterostructured nanofilm are smooth enough to neglect the boundary scattering. Thereby, three other phonon scattering mechanisms are considered in calculating the thermal conductivity, including Umklapp scattering rate τ_U, point-defect scattering rate τ_M and the acoustic

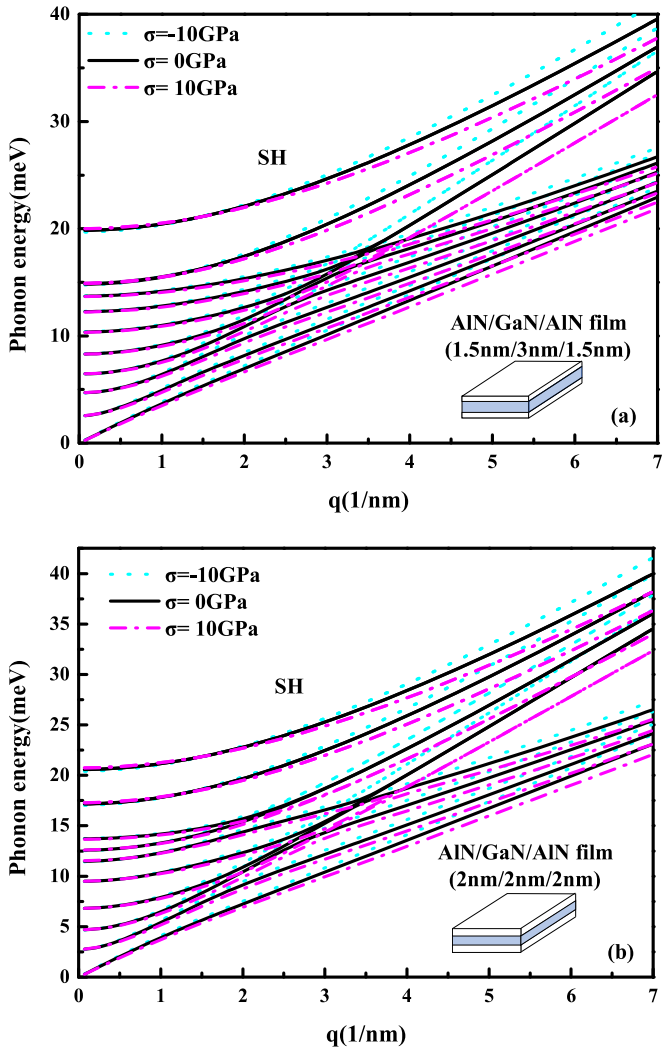

Figure 5. Phonon dispersion relations of SH mode for two typical heterostructured nanofilms under different prestress fields.

phonon-electron scattering rate τ_{ph-e}. It is well-known that the relaxation time follows the Matthiessen'rule:

$$\tau_{tot}^{-1} = \tau_U^{-1} + \tau_{ph-e}^{-1} + \tau_M^{-1}. \tag{19}$$

Thereinto, Umklaap scattering is adopted by the formula:

$$\frac{1}{\tau_U} = 2\gamma^2 \frac{k_B T}{\mu V_0} \frac{\omega^2}{\omega_D}, \tag{20}$$

where γ is Grunieisen anharmonicity parameter, V_0 is the volume per atom, and ω_D is the Debye frequency. The point-defect scattering rate can be expressed by:

$$\frac{1}{\tau_M} = \frac{V_0 \Gamma \omega^4}{4\pi V^3}. \tag{21}$$

Here, V is the phonon average group velocity, and Γ is the measure of scattering strength. The phonon-electron scattering rate at low doping level can be expressed as:

$$\frac{1}{\tau_{ph\text{-}e}} = \sqrt{\frac{\pi m^* V^2}{2k_B T}} \exp\left(-\frac{\pi m^* V^2}{2k_B T}\right) \frac{n_e \varepsilon_1^2 \omega}{\rho V^2 k_B T}, \tag{22}$$

where m^* is the electron effective mass, n_e is the concentration of conduction, ε_1 is the deformation potential, and ρ is the mass density.

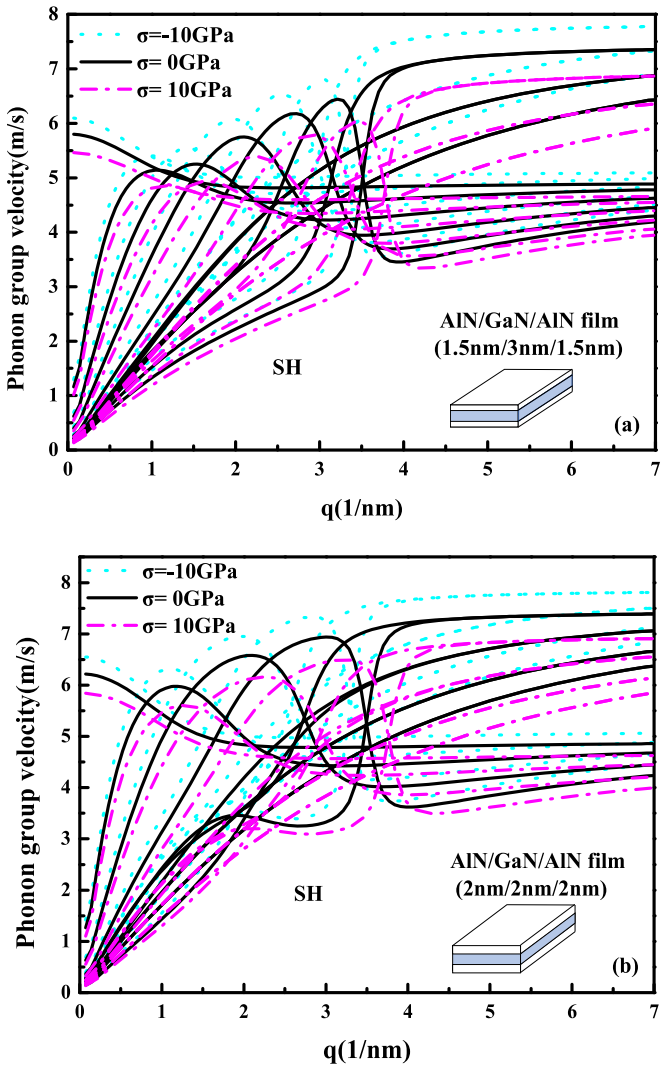

Figure 6. Phonon group velocities of SH mode for two typical heterostructured nanofilms under different prestress fields.

3. Results and discussion

3.1. Phonon properties of AlN/GaN/AlN nanofilms

In this section, the impact of heterogeneity on phonon properties of AlN/GaN/AlN nanofilms with spatially confinement effects is discussed firstly. The elastic modulus of GaN and AlN used in calculation are shown in table 1 [59, 60]. The phonon properties of wurtzite GaN and wurtzite AlN nanofilm with thickness of 6 nm, and AlN/GaN/AlN nanofilms with core layer thickness of 3 nm and 2 nm are calculated for comparison, respectively. Here, the finite different method is applied for numerical simulation with the phonon wave vector from interval $q \in (0, \ \pi/\mathrm{d})$. We take the SH mode as an example to give an insight into the phonon properties for homogenous nanofilms and heterostructured nanofilms. Figure 2 shows the phonon dispersion relations for various nanofilms. One can note that the two diagonal lines represent the dispersion relations of bulk GaN and AlN. With the increase of wave vector, the dispersion curves of homogeneous GaN and AlN nanofilms draw close to their bulk line respectively, while the dispersion curves of heterogeneous nanofilms tend to be close to the two dispersion lines of bulk. Due to the symmetry of the heterostructure, there are several lines coincide with each other. Comparing results in figures 2(a) and (b), it is not difficult to find that the phonon energy decreases with the increase of thickness of GaN layer.

Secondly, one can further calculate the phonon group velocities for SH mode, as shown in figure 3. It can be noticed from the figure that the two straight lines in figures 3(a) and (b) represent the phonon group velocity of bulk GaN and AlN. The group velocity of bulk GaN is smaller than which of bulk AlN obviously. Along with the increase of wave vector, the group velocity curves of heterostructured nanofilms gradually approach to the group

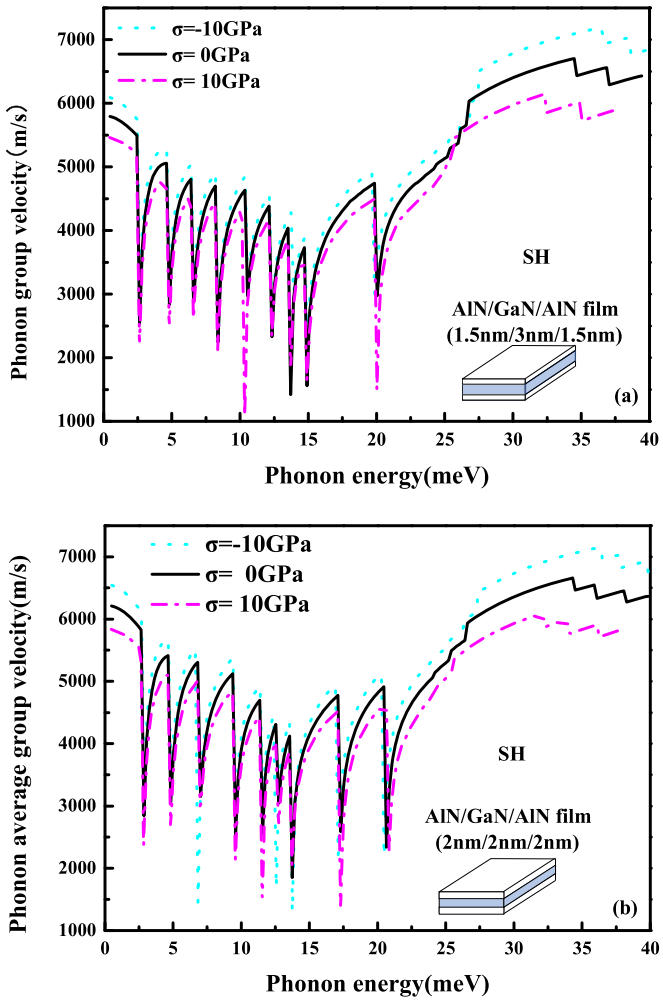

Figure 7. Phonon average group velocities of SH mode for two typical heterostructured nanofilms under different prestress fields.

velocity lines of corresponding bulk material. Different from homogeneous structures, oscillation behaviors were observed in the case of heterostructured nanofilms.

The phonon average velocities are also simulated and plotted in figure 4. Due to the spatial confinement effects, the phonon average group velocities of four structures all exhibits oscillation behaviors with the increase of phonon energy. As the GaN layer thickens, the phonon average group velocities decreases remarkably. Furthermore, figure 4(b) plots the DOS for homogenous nanofilms of GaN and AlN, and the heterostructured nanofilms with different core thicknesses. It can be found that there is higher DOS in GaN nanofilm compared with AlN nanofilm, and the peak of DOS in GaN nanofilm also appears in the region where phonon energy is lower. Comparing the DOS curves of the two heterostructures, one can find that the peak value of DOS increases with thickening the GaN layer.

3.2. Phonon properties of stressed AlN/GaN/AlN-nanofilms

In this section, the contribution of prestress fields on the phonon properties of heterostructures nanofilms is investigated in details. Figure 5 shows phonon dispersion relations of two heterostructures under different prestresses. Taking SH mode as an example, it is found that prestress has little effect on the dispersion curve when the wave vector is small. The larger wave vector is, the more obvious the influence of prestress becomes. Tensile stress reduces the phonon energy, while the compressive stress increases it. Moreover, one can find that the thinner the GaN layer is, the more significant the effect of prestress performs. Figure 6 plots the phonon group velocities of two heterostructures under different prestresses. Interestingly noted is that tensile stress reduces the group velocities while compressive one increases it. This is consistent with that in phonon dispersion relations, and the effects of prestress fields become more obvious for the case of the thinner GaN layer.

The average group velocities of two heterostructures under different prestresses are shown in figure 7. One can find that prestress fields significantly influence the average group velocity of phonons. Similarly, tensile stress makes the average velocity reduced and compressive stress make it enlarged. Figure 8 depicts the

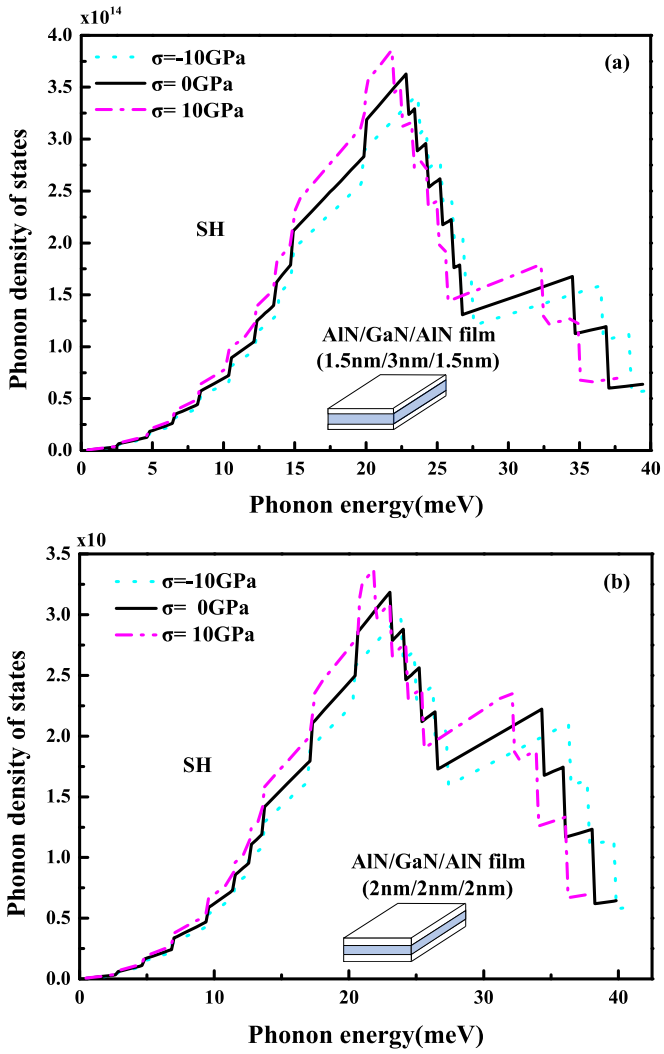

Figure 8. Phonon density of states of SH mode for two typical heterostructured nanofilms under different prestress fields.

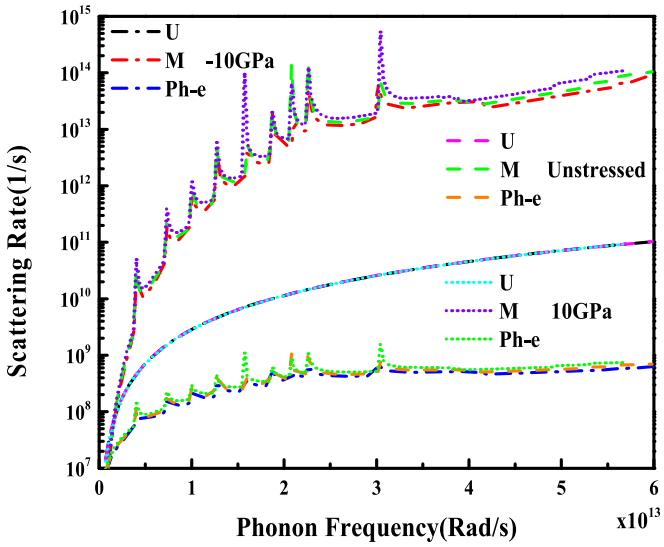

Figure 9. The variation of phonon scattering rates with phonon energy for AlN/GaN/AlN(2 nm/2 nm/2 nm) nanofilm under different prestress fields.

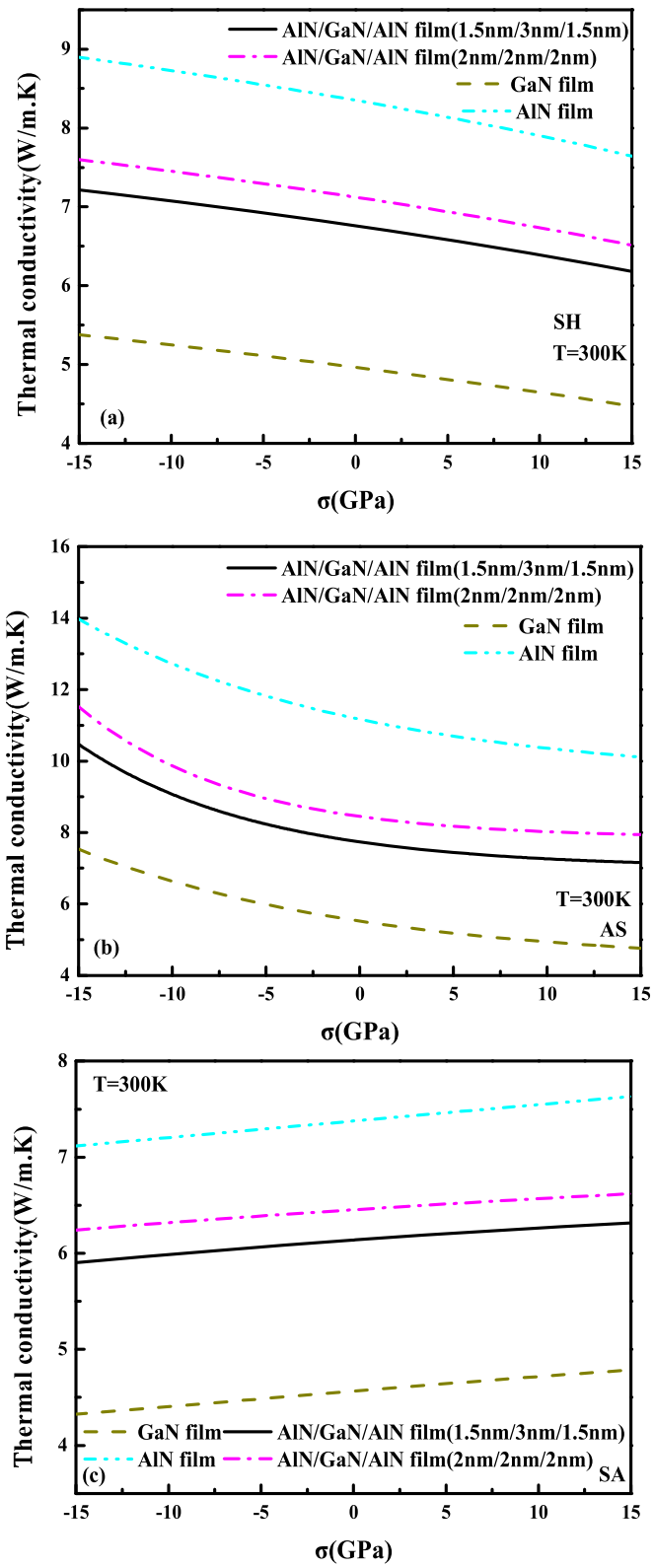

Figure 10. The variation of phonon thermal conductivity of four structured nanofilms with prestress from −15 GPa to 15 GPa at 300 K for SH mode (a), AS mode (b) and SA mode (c).

stress-dependent DOS for various heterostructured nanofilms. It can be found that tensile stress enlarges the peak value of DOS, and makes it appear in the region with lower phonon energy. The effect of compressive stress is opposite. It also can be found that the peak value of DOS has increased obviously with the thicker GaN layer by comparing the two structures.

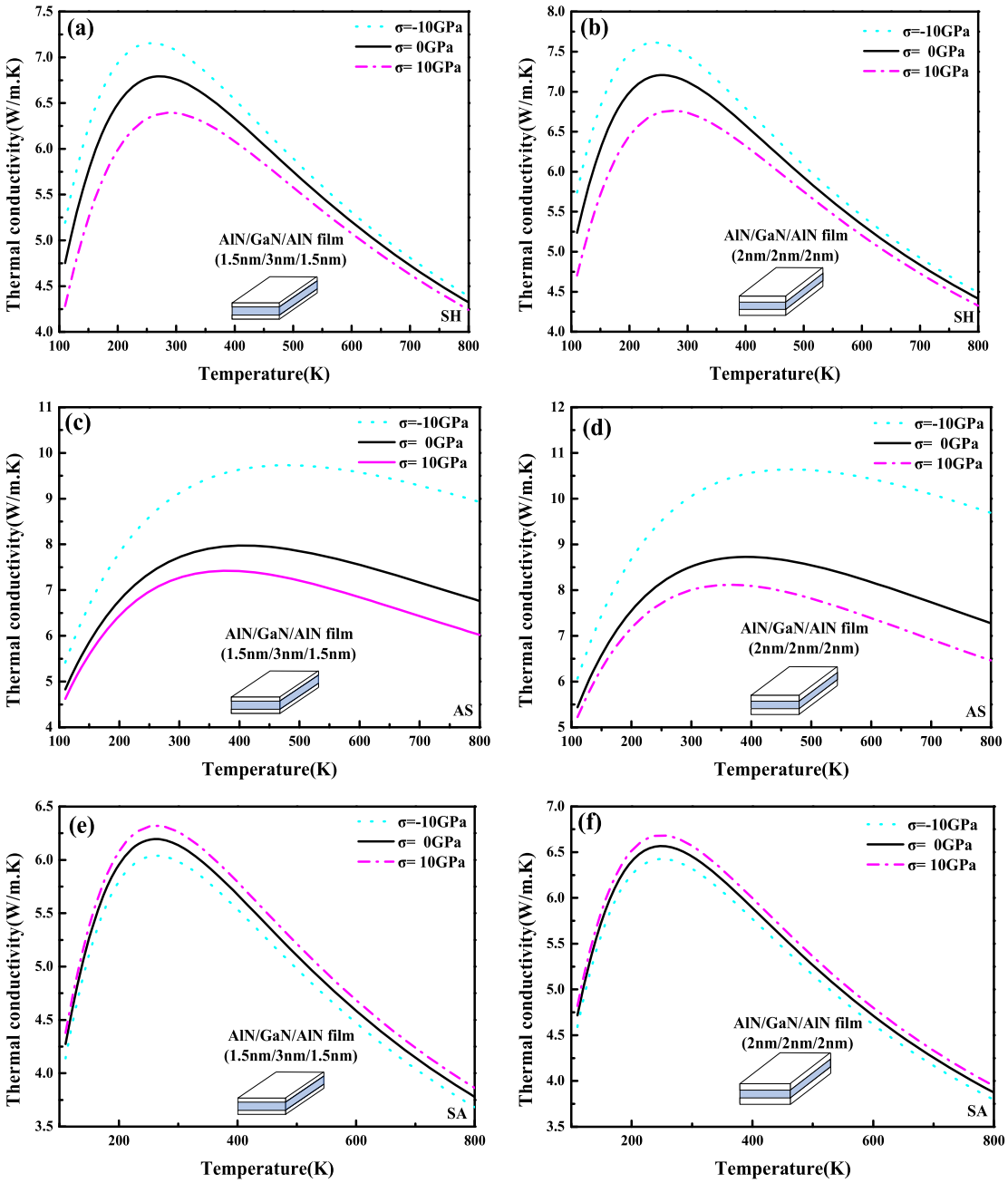

Figure 11. The variation of thermal conductivity with temperature for two typical heterostructured nanofilms under different prestresses for SH mode (a), (b), AS mode (c), (d) and SA mode (e), (f).

3.3. Phonon thermal conductivity of stressed heterostructured nanofilms.

Once the phonon group velocities and DOSs are achieved, one can calculate the various scattering rates under different prestress fields according to equations (19)–(21), including Umklapp scattering rate, point-defect scattering rate and phonon-electron scattering rate. Taking the structure of AlN(2 nm)/GaN(2 nm)/AlN(2 nm) as an example, the influence of prestress on phonon scattering rate is obtained, shown in figure 9. Obviously, the point-defect scattering is dominant, which is significantly higher than the other two scattering mechanisms. With the increase of frequency, the scattering rates increase remarkably, especially the point-defect scattering. In addition, the point-defect and phonon-electron scattering rates increase as the prestress varies from pressure to tension, but Umklaap scattering rate is almost independent on the prestress fields.

When the phonon properties and scattering rates are determined, the phonon thermal conductivity of heterostructured nanofilms can be calculated based on equations (14)–(18). Figure 10 shows phonon thermal conductivity varied with prestress fields for four structured nanofilms at 300 K. Note that the simulated phonon thermal conductivity for the pure GaN nanofilm is around 15 W mK^{-1} with the sum of conductivities of SH mode, SA mode, and AS mode. This prediction for the thermal conductivity of GaN nanofilm with the order of

10 W mK^{-1} is consistent with the ones for GaN nanostructures in literatures [61–63]. Then, we compare the thermal conductivities in four structures with different modes. It is obviously noted that GaN nanofilm has the lowest thermal conductivity, and AlN nanofilm has the highest conductivity. The thermal conductivities of heterostructures are between the conductivities of GaN nanofilm and AlN nanofilm, and decreases with thickening the GaN layer. For SH and AS modes, the thermal conductivity of four structures decreases as the prestress increases as shown in figure 9(a). For SA mode, the phonon thermal conductivities of four structures while increase with prestress as shown in figure 9(c).

Additionally, the variation of thermal conductivity with temperatures is analyzed, as shown in figure 11. Here, the prestresses are taken −10 GPa, 0 GPa and 10 GPa as examples. The phonon thermal conductivities of three modes show the same trend with increasing the temperature. That is, the conductivity rising firstly and decline later as temperature increases, and the peak value appears between 200 K and 400 K. Foer SH and AS modes, the compressive stress increases the thermal conductivity while tensile stress reduces the conductivity, which is consistent with the results above. The stress-dependent thermal conductivities of SA mode are opposite to those of SH and AS modes.

4. Conclusion

The phonon and thermal properties of stressed AlN/GaN/AlN nanofilms are investigated through considering the effects of quantum confinement and prestress fields. The acoustoelastic theory is adopted to describe the confined phonons and the contribution of prestress fields. The numerical results show that prestress can significantly change the phonon properties such as dispersion relation and group velocity, and the stress effects on the phonon properties are also sensitive to the thickness of core layer in heterostructured nanofilms. Moreover, the tensile stress reduces the phonon thermal conductivity and the compressive one increases the conductivity for SH and AS modes, which is opposite in SA mode. Prestress fields also can change the effect of temperature on thermal conductivity. It is shown that phonon properties of nanofilms can be tailored by adjusting the feature size, the value and direction of prestress, so as to regulate the thermal and electrical performance of nanostructures. This work could be useful for thermal management in nano/microelectronic devices and the rational design and optimization of high-performance semiconductor-based electronic devices.

Acknowledgments

This research is supported by the National Natural Science Foundation of China (Grant nos. 11772294, 11621062, 11302189), and the Fundamental Research Funds for the Central Universities (Grant no. 2017QNA4031). W Y Yin acknowledges the support from the National Natural Science Foundation of China (Grant no. 61431014).

ORCID iDs

Linli Zhu https://orcid.org/0000-0002-5178-877X

References

[1] Tong X C 2011 *Advanced Materials for Thermal Management of Electronic Packaging* (Berlin: Springer) pp 39–65
[2] Ferain I, Colinge C A and Colinge J P 2011 Multigate transistors as the future of classical metal-oxide-semiconductor field-effect transistors *Nature* **479** 310–6
[3] Moore A L and Shi L 2014 Emerging challenges and materials for thermal management of electronics *Mater. Today* **17** 163–74
[4] Nasri F, Aissa M F B and Belmabrouk H 2017 Nanoheat conduction performance of black phosphorus field-effect transistor *IEEE T. Electron. Dev.* **64** 2765–9
[5] Cahill D G *et al* 2003 Nanoscale thermal transport *J. App. Phys.* **93** 793–818
[6] Bachmann C and Bar-Cohen A 2008 A Hotspot remediation with anisotropic thermal interface materials *Intersociety Conf. on Thermal and Thermomechanical Phenomena in Electronic Systems Itherm* pp 238–47
[7] Guo Y and Wang M 2015 Phonon hydrodynamics and its applications in nanoscale heat transport *Phys. Rep.* **595** 1–44
[8] Rezgui H *et al* 2018 Modeling thermal performance of nano-GNRFET transistors using ballistic-diffusive equation *IEEE T. Electron. Dev.* **65** 1611–6
[9] Zevalkink A, Toberer E S, Zeier W G, Espen F L and Snyder G J 2011 Ca_3AlSb_3: an inexpensive, non-toxic thermoelectric material for waste heat recovery *Energ. Environ. Sci.* **4** 510–8
[10] Maneewan S, Khedari J, Zeghmati B, Hirunlabh J and Eakburanawat J 2003 Investigation on generated power of thermoelectric roof solar collector *Renew. Energ.* **29** 743–52
[11] Rowe D 2006 *Thermoelectrics Handbook: Macro to Nano* (Boca Raton FL: CRC Press) (https://doi.org/10.1201/9781420038903)
[12] Song E *et al* 2016 Enhanced thermoelectric transport in modulation-doped GaN/AlGaN core/shell nanowires *Nanotechnology* **27** 015204

[13] Nika D L *et al* 2011 Reduction of lattice thermal conductivity in one-dimensional quantum-dot superlattices due to phonon filtering *Phys. Rev.* B **84** 165415
[14] Hicks L D and Dresselhaus M S 1993 Effect of quantum-well structures on the thermoelectric figure of merit *Phys. Rev.* B **47** 12727
[15] Nolas G S, Sharp J and Goldsmid E H J 2001 *Thermoelectrics* (Berlin: Springer) (https://doi.org/10.1007/978-3-662-04569-5)
[16] Balandin A and Wang K L 1998 Effect of phonon confinement on the thermoelectric figure of merit of quantum wells *J. App. Phys.* **84** 6149–53
[17] Casian A, Sur I, Scherrer H and Dashevsky Z 2000 Thermoelectric properties of n-type PbTe/$Pb_{1-x}Eu_xTe$, quantum wells *Phys. Rev.* B **61** 15965–74
[18] Kondow M, Uomi K, Hosomi K and Mozume T 1994 Gas-source molecular beam epitaxy of GaN_xAs_{1-x} using a N radical as the N source *Jpn. J. Appl. Phys.* **33** L1056–8
[19] Kondow M, Kitatani T, Nakatsuka S and Larson M C 1997 GaInNAs: a novel material for long-wavelength semiconductor lasers *IEEE J. Sel. Top. Quant.* **3** 719–30
[20] Kasper E and Paul D J 2005 *Heterostructure Bipolar Transistors-HBTs* (Berlin: Springer) (https://doi.org/10.1007/3-540-26382-9_6)
[21] Jiang C *et al* 2017 Piezotronic effect tuned AlGaN/GaN high electron mobility transistor *Nanotechnology* **28** 455203
[22] Mishra U K, Parikh P and Wu Y F 2002 AlGaN/GaN HEMTs-an overview of device operation and applications *Proc IEEE* **90** 1022–31
[23] Minj A, Cavalcoli D and Cavallini A 2012 Thermionic emission from the 2DEG assisted by image-charge-induced barrier lowering in AlInN/AlN/GaN heterostructures *Nanotechnology* **23** 115701
[24] Borca-Tasciuc T *et al* 2001 Thermal conductivity of InAs/ AlSb superlattices *Nanosc. Microsc. Therm.* **5** 225–31
[25] Zeng T and Gang C 2003 Nonequilibrium electron and phonon transport and energy conversion in heterostructures *Microelectron. J.* **34** 201–6
[26] Nika D L, Zincenco N D and Pokatilov E P 2009 Engineering of thermal fluxes in phonon mismatched heterostructures *J. Nanoelectron. Optoelectron.* **4** 180–5
[27] Zincenco N D, Nika D L, Pokatilov E P and Balandin A A 2007 Acoustic phonon engineering of thermal properties of silicon-based nanostructures *J. Phys.: Conf. Ser.* **92** 012086–9
[28] Nika D L, Zincenco N D and Al-Sabayleh M 2006 Acoustical properties of rectangular GaN quantum wires covered by elastically dissimilar barries with clamped outer surfaces *Moldavian J. Phys. Sci.* **5** 103–12
[29] Narendra N and Kim K W 2017 Toward enhanced thermoelectric effects in Bi_2Te_3/Sb_2Te_3 heterostructures *Semicond. Sci. Tech.* **32** 035005
[30] Pokatilov E P, Nika D L and Balandin A A 2003 Phonon spectrum and group velocities in AlN/GaN/AlN and related heterostructures *Superlattice. Microst.* **33** 155–71
[31] Jaccodine R J and Schlegel W A 1966 Measurement of strains at Si–SiO_2 interface *J. Appl. Phys.* **37** 2429–34
[32] Brantley W A 1973 Calculated elastic constants for stress problems associated with semiconductor devices *J. Appl. Phys.* **44** 534–5
[33] Woo S Y *et al* 2015 Interplay of strain and indium incorporation in InGaN/GaN dot-in-a-wire nanostructures by scanning transmission electron microscopy *Nanotechnology* **26** 344002
[34] Taylor T C and Yuan F L 1962 Thermal stress and fracture in shear-constrained semiconductor device structures *IRE T. Electron. Dev.* **9** 303–8
[35] Bai J G, Zhang Z Z, Calata J N and Lu G Q 2006 Low-temperature sintered nanoscale silver as a novel semiconductor device-metallized substrate interconnect material *IEEE T. Compon. Pack. T.* **29** 589–93
[36] Ross R G, Andersson P, Sundqvist B and Backstrom G 1984 Thermal conductivity of solids and liquids under pressure *Rep. Prog. Phys.* **47** 1347
[37] Sui Z and Herman I P 1993 Effect of strain on phonons in Si, Ge, and Si/Ge heterostructures *Phys. Rev.* B **48** 17938
[38] Ghanbari R A *et al* 1990 Phonon frequencies for Si–Ge strained-layer superlattices calculated in a three-dimensional model *Phys. Rev.* B **42** 7033
[39] Li X, Maute K, Dunn M L and Yang R 2010 Strain effects on the thermal conductivity of nanostructures *Phys. Rev.* B **81** 245318
[40] Bhowmick S and Shenoy V B 2006 Effect of strain on the thermal conductivity of solids *J. Chem. Phys.* **125** 234
[41] Paul A and Klimeck G 2011 Strain effects on the thermal properties of ultra-scaled Si nanowires *Appl. Phys. Lett.* **99** 383
[42] Zhu L L and Zheng X J 2009 Modification of the phonon thermal conductivity in spatially confined semiconductor nanofilms under stress fields *EPL* **88** 36003
[43] Zhu L L and Ruan H H 2014 Influence of prestress fields on the phonon thermal conductivity of GaN nanostructures ASME- *J. Heat Transf.* **136** 102402
[44] Zhu L L and Luo H N 2016 Phonon properties and thermal conductivity of GaN nanofilm under prestress and surface/interface stress *J. Alloy. Compd.* **685** 619–25
[45] Wang J, Zhu L and Yin W 2018 Effects of heterogeneity and prestress field on phonon properties of semiconductor nanofilms *Comp. Mater. Sci* **145** 14–23
[46] Picu R C, Borcatasciuc T and Pavel M C 2003 Strain and size effects on heat transport in nanostructures *J. Appl. Phys.* **93** 3535–9
[47] Paul A and Klimeck G 2011 Strain effects on the thermal properties of ultra-scaled Si nanowires *Appl. Phy. Lett.* **99** 383
[48] Broido D A and Reinecke T L 1998 Thermoelectric transport in quantum well superlattices *Appl. Phys. Lett.* **70** 2834–6
[49] Borca-Tasciuc T *et al* 2000 Thermal conductivity of symmetrically strained Si/Ge superlattices *Superlattice. Microstruct.* **28** 199–206
[50] Ren S F, Cheng W and Chen G 2006 Lattice dynamics investigations of phonon thermal conductivity of Si/Ge superlattices with rough interfaces *J. Appl. Phys.* **100** 203–59
[51] Bannov N, Aristov V V, Mitin V V and Stroscio M A 1995 Electron relaxation times due to the deformation-potential interaction of electrons with confined acoustic phonons in a free-standing quantum well *Phys. Rev.* B **51** 9930–42
[52] Bornemann A 1998 Significant decrease of the lattice thermal conductivity due to phonon confinement in a free-standing semiconductor quantum well *Phys. Rev.* B **58** 1544–9
[53] Osetrov A V, Fröhlich H J, Koch R and Chilla E 2000 Acoustoelastic effect in anisotropic layered structures *Phys. Rev.* B **621** 13963–9
[54] Zou J, Lange X and Richardson C 2006 Lattice thermal conductivity of nanoscale AlN/GaN/AlN heterostructures: effects of partial phonon spatial confinement *J. Appl. Phys.* **100** 89–96
[55] Martin P, Aksamija Z, Pop E and Ravaioli U 2009 Impact of phonon-surface roughness scattering on thermal conductivity of thin Si nanowires *Phys. Rev. Lett.* **102** 125503
[56] Chen G 1998 Thermal conductivity and ballistic-phonon transport in the cross-plane direction of superlattices *Phys. Rev.* B **57** 14958–73
[57] Hou Y and Zhu L L 2016 Influence of surface scattering on the thermal properties of spatially confined gan nanofilm *Chinese Phys.* B **25** 86502

[58] Ran X, Guo Y and Wang M 2018 Interfacial phonon transport with frequency-dependent transmissivity by Monte Carlo simulation *Int. J. of Heat and Mass Trans.* **123** 616–28
[59] Łepkowski S P 2005 Nonlinear elasticity in III-N compounds: *ab initio* calculations *Phys. Rev.* B **72** 245201
[60] Łepkowski S P and Gorczyca I 2011 *Ab initio* study of elastic constants in $In_xGa_{1-x}N$ and $In_xAl_{1-x}N$ wurtzite alloys *Phys. Rev.* B **83** 203201
[61] Wang Z, Zu X, Gao F and Weber W J 2007 Atomistic simulation of the size and orientation dependences of thermal conductivity in GaN nanowires *Appl. Phys. Lett.* **90** 161923
[62] Zhou X W, Jones R E and Aubry S 2010 Molecular dynamics prediction of thermal conductivity of GaN films and wires at realistic length scales *Phys. Rev.* B **81** 155321
[63] Zhou G and Li L 2012 Phonon thermal conductivity of GaN nanotubes *J. Appl. Phys.* **112** 014317